

INVESTIGATION OF THE CRITICAL RF FIELDS OF SUPERCONDUCTING CAVITY CONNECTIONS*

J. C. Wolff^{1†}, J. Iversen, D. Klinke, D. Kostin, D. Reschke, S. T. Sievers, A. Sulimov, J.-H. Thie, M. Wiencek, Deutsches Elektronen-Synchrotron, Notkestraße 85, D-22607 Hamburg, Germany
R. Wendel, ¹HAW Hamburg, Berliner Tor 7, D-20099 Hamburg, Germany

Abstract

To optimise the length of the drift tube of a superconducting cavity (SC), it is required to know the critical value of the RF fields to prevent a potential early quench at the flange connection in case of a drift tube length reduction. To avoid changes on the SC which has been used for the tests, all RF cryogenic experiments have been carried out by using a cylinder in the center of a 1-cell cavity drift tube to increase the field magnitude at the connection. This cylinder has been designed and optimised by RF simulations to provide a field density at the connection twice as high as at a chosen reference point near the iris. Hence also a test SC with a comparatively low gradient can be used without causing field restrictions. In this contribution an approach to investigate the field limitations of 1.3 GHz TESLA-Shape SC connections and thereby the minimal drift tube length based on simulations will be presented.

INTRODUCTION

For the development of future accelerator components the ongoing work investigates the field limitation for commonly used connections shown in Fig. 1 originally designed for low field areas as well as cost efficient approaches to increase the critical magnitudes in the connection region. Since the cut-off frequency of the drift tube is higher than its fundamental mode frequency, the electromagnetic field along the drift tube decreases exponentially as shown in Fig. 2. Due to the low field magnitude at the current position of the connection there are just marginal and hence uncritical losses.

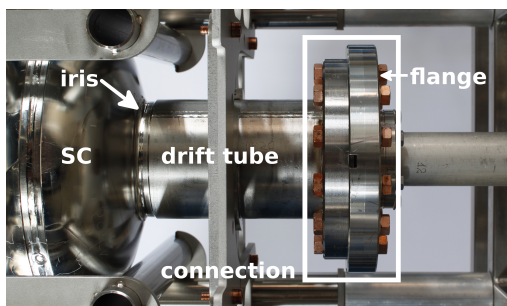


Figure 1: Commonly used connection design for low field areas.

In case of a stepwise drift tube length reduction the field strength increases and therefore the losses in the normal

conducting vacuum gasket would yield at some point to a premature quench in the connection region.

To avoid any changes on the test cavity, a cylinder in the center of the drift tube has been used to turn it into a coaxial line. By this modification the field density at the connection can be increased and the connection can be virtually displaced. In this way the drift tube length limitation can be found by increasing the RF power stepwise until the breakdown occurs in the connection region. A subsequent comparison of the measurements with an appropriate simulation model will yield to the desired critical field magnitudes as well as the minimal distance between the connection and the iris.

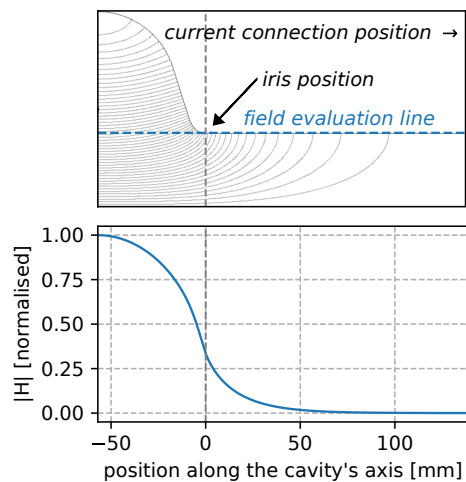


Figure 2: Exponential decay along the drift tube.

Field limitations for different vacuum gasket types and materials had already been previously investigated in 1976 at the Kernforschungszentrum Karlsruhe as an attempt to develop a superconducting connection for the use in a SRF particle separator for CERN. Ring-shaped gaskets made of niobium or lead had been tested, but showed either high losses or caused grooves on the connection surfaces. At last a design separating the functions of the RF contacting and the UHV-tightness could be successfully tested at a magnetic flux of $\sim 3 - 5$ mT [1]. A good RF contact had been established by special shaped "lips" to break through the oxide layer of the flange surfaces during the mounting process. UHV-tightness had been ensured by indium wires between each flange and the niobium gasket [2].

Later attempts for connections able to withstand a magnetic flux of up to 30 mT (for the use in a superstructure configuration) had been developed at DESY and Jeffer-

* This work was supported by the Helmholtz Association within the topic Accelerator Research and Development (ARD) of the Matter and Technologies (MT) Program.

† jonas.wolff@desy.de

son Lab. Since commonly used NbTi55 (according to XFEL specification [3]) flanges have a low critical flux of ~ 10 mT [4] and a comparatively low thermal conductivity of $\sim 0.05 \text{ W m}^{-1} \text{ K}^{-1}$ [5] a Nb-1Zr alloy had been considered for the flanges together with a vacuum gasket made of ultra pure niobium to realise the connection [1, 6].

DESIGN DEVELOPMENT

The coaxial line has been designed to provide a field density at the connection gap twice as high as at a chosen reference point 30 mm afar from the iris marked in Fig. 2. This reference point should represent a realistic minimum for the flange position because for the mounting process some additional space is needed to avoid a possible damage of the nearby cell. By choosing a higher field density also a test cavity with a comparatively low gradient can be used. To preserve the possibility of a later upgrade to a double-walled and thereby actively helium cooled version for the cylinder insert a inner diameter of 21 mm and a material thickness of 3 mm has been chosen.

Due to axial symmetry, the LAACG Poisson Superfish group of codes has been used for the development. The optimal cylinder length was found by the bisection method implemented in an external C-program. This program automatised the numerous geometry changes and the related data evaluation. By analysing the field distribution at the inner surface of the drift tube alongside the cavity's axis, an unwanted impact on the distribution at the power couplers drift tube and the cells field could be ruled out as shown in Fig. 3. Due to the more descriptive images, an appropriate CST Microwave Studio model was used for the field visualisation. The cylinder was made of niobium with a residual resistance ratio (RRR) of 47. A CAD model and the finished cylinder manufactured by Ettore Zanon S.p.A. is shown in Fig. 4. Since for the flange socket a higher material hardness is required, a NbTi55 alloy was used.

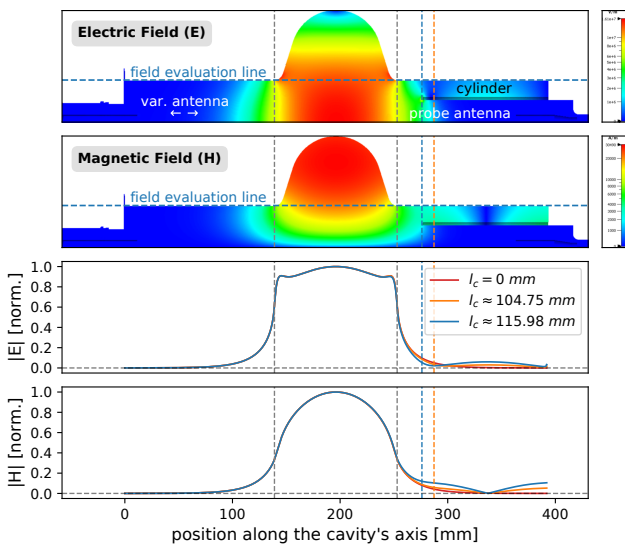


Figure 3: Impact on the cavity's field distribution by different lengths l_c of the added coaxial line.

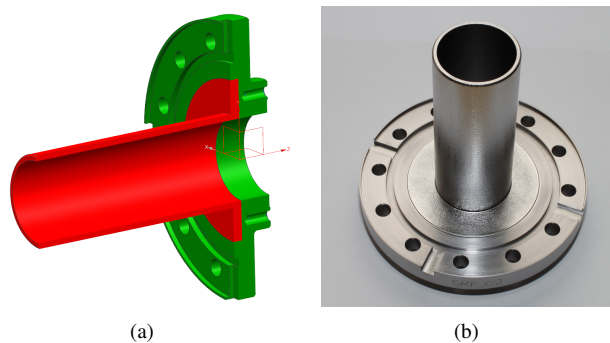


Figure 4: CAD model of the cylinder insert (a), finished cylinder insert before the assembly (b).

MODEL VALIDATION

Due to the differences of the field distribution in a coaxial line and a wave guide driven below its cut-off frequency, possible deviations had to be investigated, to ensure that the model maps the behavior at different connection positions correctly. It could be shown, that the radial magnetic field distribution in the connection gap is almost identical for both propagation cases (Fig. 5).

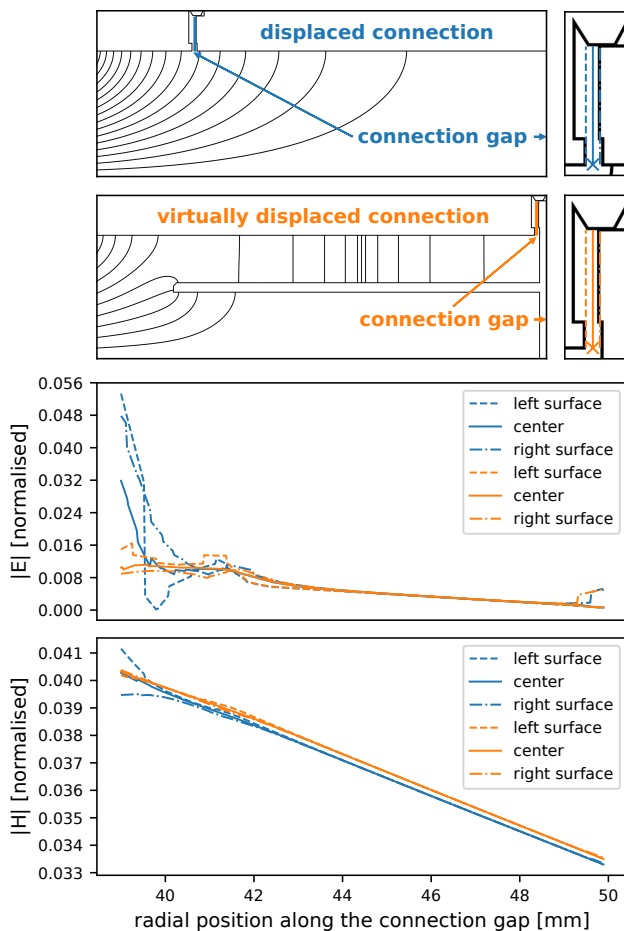
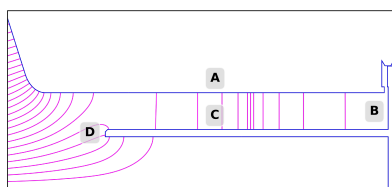


Figure 5: Field deviations inside of the connection gap.

Content from this work may be used under the terms of the CC BY 3.0 licence (© 2019). Any distribution of this work must maintain attribution to the author(s), title of the work, publisher, and DOI.

The density decays largely linear alongside the gap except for areas close to the flange surfaces in the gap entrance. This effect has been taken into account by the positioning of the reference points. By setting them to the center of the gap entrance, an error caused by these non linearities could be avoided. In a simulation results comparison of an empty (reference) cavity and a model including the coaxial line the relative error for the TM_{010} resonant frequency and field magnitudes were $< 0.1\%$ and hence neglectable for this application.

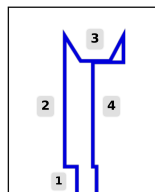
After altering the field distribution in the drift tube by the coaxial line, the distribution of the proportional losses (prob. l.) changed for the surface Segments (Seg.) in Fig. 6. The recorded changes allowed an investigation of the impact on the cavity's quality factor. Furthermore the losses on the cylinder surface were studied since they may limit the maximum field density. In an empty cavity the inner drift tube surface (Segment A) has proportional losses of $\sim 0.1528\%$ of the total setup's power losses.



Seg.	prop. l.
A	0.2874 %
B	0.0412 %
C	0.1761 %
D	0.0052 %

Figure 6: Proportional surface losses for each surface region.

We investigated the proportional surface losses for each region (Reg.) of the connection shown in Fig. 7 as well. Thus, the impact on the quality factor by different gasket and flange materials can be determined and potential quench causing regions may be spotted. An investigation of the impact on the quality factor is especially important for the use of normal conducting aluminium gaskets (Fig. 7 Reg. 3), since a high surface impedance may suppress impedance matching within the input coupler's antenna adjustment range.



Reg.	prop. l.
1	0.0068 %
2	0.0197 %
3	0.0126 %
4	0.0213 %

Figure 7: Regions of the connection gap assigned in dependence of the particular materials.

POWER COUPLING

To ensure that impedance matching can be established for all vertical tests, the external quality factor has been simulated by CST Microwave Studio as a function of the antenna penetration depth. The simulation results have been verified by comparing them with the measurements. As shown in Fig. 8 there is just a small deviation between the simulation and the measurements.

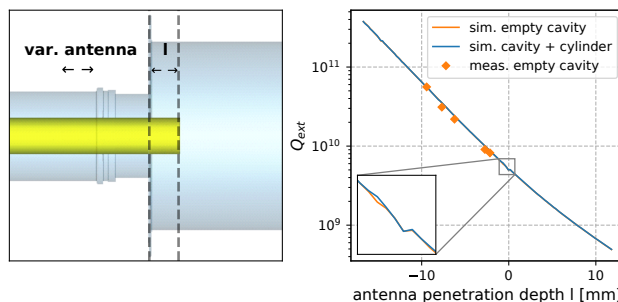


Figure 8: Q_{ext} of the input antenna as a function of its penetration depth.

Low deviations between the simulation and the measurements are especially important for the development of a new field probe antenna design. Since the inner cylinder diameter is extensively smaller than the drift tube's diameter, the exponential decay of the field density is respectively higher. Therefore the normally used probe antenna had to be replaced by a new design to achieve a desired quality factor of $2.5 \cdot 10^{12}$. This value is a compromise between a higher impact of the background noise to the measured signal and preferably low power losses and thereby a low influence on the setup's field distribution.

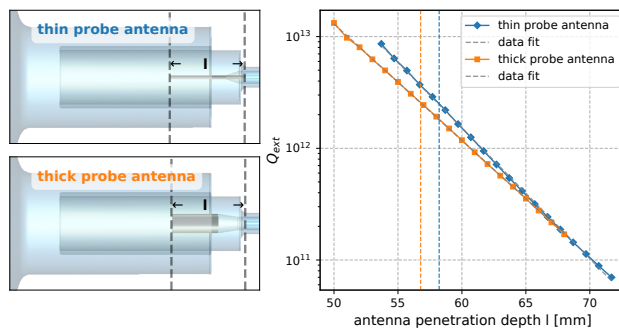


Figure 9: Q_{ext} of the field probe antenna as a function of the penetration depth.

For the field probe antenna two approaches have been investigated (Fig. 9). The first one, the "thin probe antenna", has been designed to provide a low sensitivity on length aberrations. The second one, the "thick probe antenna" is a shortened version of the adjustable antenna for the power coupling and therefore a cost efficient approach. Since the sensitivity differences between both designs are low, the thick version has been produced at DESY.

VERTICAL TESTING

A first vertical test investigated the field limitation for normal conducting aluminium gaskets. As shown in the Q_0 vs. E_{acc} curve in Fig. 10, the losses at the gaskets surface led to a significant decrease of the quality factor in comparison to an empty cavity and the quench occurred already at ~ 4 MV/m.

During the vertical tests a direct measurement of the field magnitude in the connection gap was not possible. Therefore

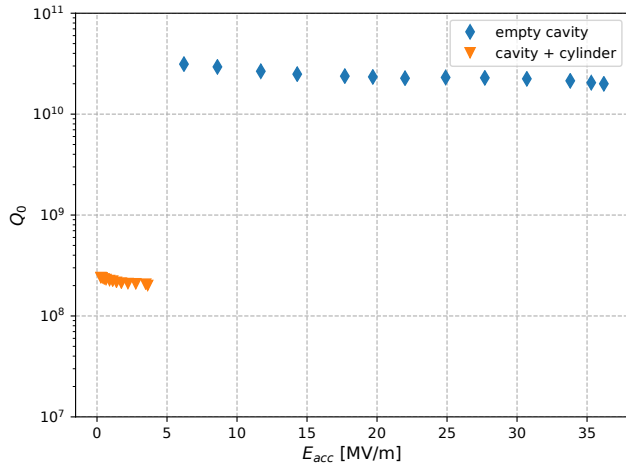


Figure 10: Q_0 vs. E_{acc} curve.

the field magnitude had to be calculated on basis of the effective accelerating field E_{acc} measured as specified in [7] and the simulation model as follows. For the simulations E_{acc} can be computed by:

$$E_{acc} = \frac{1}{l_{cell}} \int_0^{l_{cell}} E_z(z) \cos(\phi) dz, \quad (1)$$

where $\phi = \frac{\omega \cdot z}{c_0} - \phi_0$

The offset ϕ_0 represents the time an accelerated electron needs for the distance between the flange and the center of the cell to experience the maximum possible acceleration under the simplified assumption the electron travels with the vacuum speed of light c_0 . We can simplify the analysis by operating with the simulated maximal electric field in the cavity E_{max} . Both, E_{acc} and E_{max} depend on the stored energy in the cavity. Therefore the ratio between E_{max} and E_{acc} does not depend on the normalisation and can be found by:

$$k = \frac{E_{max}}{E_{acc}} \quad (2)$$

For the used model: $W = 48.7$ mJ, $E_{acc} = 2.03$ MV/m and $E_{max} = 3.55$ MV/m a factor $k = 1.75$ has been calculated. Hence E_{max} of the vertical test is ~ 7 MV/m. Then the critical magnetic field density in the center of the gap entrance can be calculated by a factor p depending on the length of the coaxial line (In the presented case $p = 1.368 \cdot 10^{-4} \Omega^{-1}$) as follows:

$$H_{con}[A/m] = E_{max}[V/m] \cdot p[\Omega^{-1}] \quad (3)$$

This approach leads to a critical magnetic field density of $\sim 9.576 \cdot 10^2$ A/m and a critical magnetic flux of ~ 1.2 mT. The dependence of E_{max} and H_{con} or B_{con} is shown Fig. 11.

The minimal distance between the iris and the connection gap ($l_{drift\ tube}$) can be found by an iterativ comparison of p with the particular element of the H-value array of the

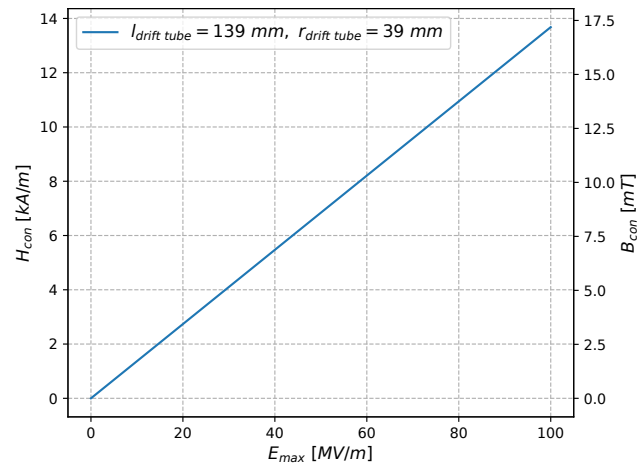


Figure 11: H_{con} as a function of E_{max} .

field evaluation line in Fig. 2 normalised by the product of $1/E_{max_simulation}$ and the ratio $E_{breakdown}/E_{max_measurement}$. Whereat $E_{breakdown}$ equates the maximum possible E-field density of the test cavity depending on the individual gradient. For the presented case and a known value $E_{breakdown}$ the minimal drift tube length can be read from the plot in Fig. 12. For a critical magnetic flux of ~ 1.2 mT this leads to a minimal distance of ~ 65.6 mm.

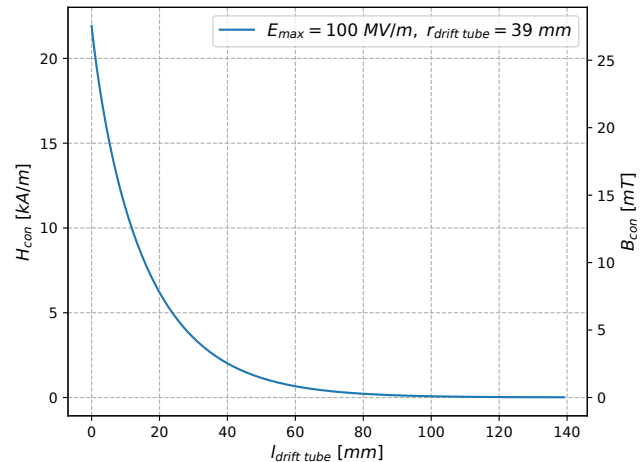


Figure 12: H_{con} as a function of $l_{drift\ tube}$.

As an attempt to detect an asymmetrical temperature increase a thermometry system as described in [8] based on calibrated carbon resistors has been used. Fig. 13 shows the mounted sensors on the blind flange in vicinity of the vacuum gaskets. Due to the high material thickness of both flanges and the low gradient no temperature changes above the mean measurement error of ~ 3.7 mK could be measured. Only by increasing the input power by almost 20 times a small temperature change of ~ 6 mK could be measured with two sensors close to the probe antenna's gasket.

Especially for superconducting connections which are able to withstand remarkably higher fields it cannot be ruled

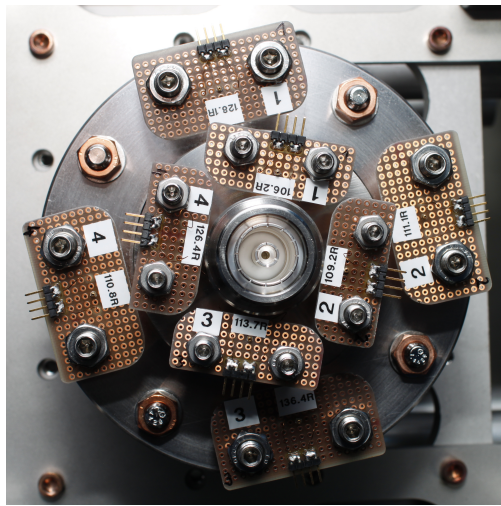


Figure 13: Arrangement of the mounted temperature sensors in vicinity of the vacuum gaskets.

out that the surface of the cylinder insert may be the field limiting factor. Therefore in the further vertical tests a second sound quench detection system will be used as an attempt to locate the field limiting region.

CONCLUSION

To investigate the field limitation for the gap area of SC connections in case of a remarkable drift tube length reduction, a superconducting cylinder was longitudinally mounted in the center of a test cavity's drift tube. By this modification the drift tube was turned into a coaxial line to increase the field density in the connection gap and thereby virtually displace the transition without any changes on the test cavity. The plausibility of this model has been checked by RF simulations. It could be shown that the impact on the TM_{010} resonant frequency, the external quality factor and the field distribution in the connection gap is neglectably low. In a first vertical test with a normal conducting aluminium gasket, the measurement setup showed a low quality factor of $3 \cdot 10^8$ and a low gradient of ~ 4 MV/m which corresponds to a magnetic flux at the connection gap of ~ 1.2 mT and a minimal distance between the iris and the connection gap of ~ 65.6 mm under the assumption that the gap is the field limiting element of the setup.

Temperature sensors mounted on the blind flanges close to the vacuum gaskets were used as an attempt to detect an asymmetrical temperature increase. Due to the low input

power and the high material thickness of the flanges no signal ahead of the parasitic error could be measured.

As an approach to spot the quench region and thereby hopefully rule out that the cylinder surface is the limiting factor a second sound quench detection system will be used.

To increase the critical fields in the connection gap an attempt to shield the gap by a niobium RF seal will be tested in the near future.

ACKNOWLEDGEMENT

We would like to thank our colleagues - T. Büttner, C. Ceylan, N. Engling, A. Ermakov, K. Lando, W.-D. Möller, C. Müller, A. Muhs, M. Schmökel, L. Steder and B. van der Horst from DESY and W. Hillert from the University of Hamburg - for their support of this work as well the manufacturer Ettore Zanon S.p.A. for the development of the etching system.

REFERENCES

- [1] P. Kneisel, G. Ciovati, J. Sekutowicz, A. Matheisen, X. Singer, W. Singer, "Development of a Superconducting Connection for Niobium Cavities", in *Proc. PAC'07*, Albuquerque, NM, USA, Jun. 2007, paper WEPMS062, pp. 2484–2486.
- [2] M. Grundner, H. Lengeler, E. Rathgeber, "RF Contact for Superconducting Resonators", *Nuclear Instruments and Methods*, vol. 141, no. 1, pp. 57–59, 1977.
- [3] Technical Specifications, Nb55Ti Alloy, Technical Report Revision C, May 07 2010, XFEL/008.
- [4] S. Giordano, H. Hahn, H. Halama, T. Luhman, and W. Bauer, "Investigation of Microwave Properties of Superconducting Nb_{0.4}Ti_{0.6}", *IEEE Transactions on Magnetics*, vol. 11, no. 2, pp. 437–440, March 1975.
- [5] E. W. Collings, *Applied Superconductivity, Metallurgy, and Physics of Titanium Alloys*, New York, USA, Plenum Press, 1986.
- [6] R. Bandelmann, G. Ciovati, J. Sekutowicz, A. Matheisen, X. Singer, and W. Singer, "Nb Prototype of the Superstructure for the TESLA Linear Collider", pp. 490–493, 1999.
- [7] H. Padamsee, J. Knobloch, and T. Hays, "RF Superconductivity for Accelerators", Weinheim, Germany, WILEY-VCH Verlag, 2008.
- [8] J. Knobloch, H. Muller, and H. Padamsee, "Design of a High Speed, High Resolution Thermometry System for 1.5 GHz Superconducting Radio Frequency Cavities" *Review of Scientific Instruments*, vol. 65, pp. 3521–3527, 1994.